

Ferromagnetic quantum phase transition in Sr_{1-x}CaxRuO₃ thin films

M. Schneider, V. Moshnyaga, Philipp Gegenwart

Angaben zur Veröffentlichung / Publication details:

Schneider, M., V. Moshnyaga, and Philipp Gegenwart. 2010. "Ferromagnetic quantum phase transition in Sr_{1-x}CaxRuO₃ thin films." *physica status solidi (b)* 247 (3): 577–79.
<https://doi.org/10.1002/pssb.200983004>.

Nutzungsbedingungen / Terms of use:

licgercopyright

Dieses Dokument wird unter folgenden Bedingungen zur Verfügung gestellt: / This document is made available under these conditions:

Deutsches Urheberrecht

Weitere Informationen finden Sie unter: / For more information see:

<https://www.uni-augsburg.de/de/organisation/bibliothek/publizieren-zitieren-archivieren/publiz/>



Ferromagnetic quantum phase transition in $\text{Sr}_{1-x}\text{Ca}_x\text{RuO}_3$ thin films

M. Schneider, V. Moshnyaga, and P. Gegenwart*

I. Physikalisches Institut, Georg-August-Universität Göttingen, Friedrich-Hund-Platz 1, 37077 Göttingen, Germany

*Corresponding author: e-mail pgegenw@gwdg.de, Phone: +49 551 397607, Fax: +49 551 3919546

The ferromagnetic (FM) quantum phase transition in the perovskite ruthenate $\text{Sr}_{1-x}\text{Ca}_x\text{RuO}_3$ is studied by low-temperature magnetization and electrical resistivity measurements on thin films. The films were grown epitaxially on SrTiO_3 substrates using metalorganic aerosol deposition and characterized by X-ray diffraction and room temperature scanning tunneling microscopy. High residual resistivity ratios of 29 and 16 for $x = 0$ and 1, respectively, prove the high quality of the

investigated samples. We observe a continuous suppression of the FM Curie temperature from $T_C = 160$ K at $x = 0$ towards $T_C \rightarrow 0$ at $x_c \approx 0.8$. The analysis of the electrical resistivity between 2 and 10 K reveals T^2 and $T^{3/2}$ behavior at $x \leq 0.6$ and $x \geq 0.7$, respectively. For undoped CaRuO_3 , the measurement has been extended down to 60 mK, revealing a crossover to T^2 behavior around 2 K, which suggests a Fermi-liquid ground state in this system.

1 Introduction Quantum phase transitions (QPTs) in weak itinerant ferromagnets have recently attracted much interest due to the discovery of exciting low-temperature states such as unconventional superconductivity [1], partial magnetic order [2], or non-Fermi liquid (NFL) phases [3]. The system $\text{Sr}_{1-x}\text{Ca}_x\text{RuO}_3$ represents a rare example of an oxide NFL metal that displays an itinerant electron ferromagnetic (FM) QPT [4–6]. Although the general trend of a continuous suppression of ferromagnetism with increasing Ca concentration is well established, details close to the QPT differ substantially in previous reports. Early studies on sintered polycrystals have suggested a FM quantum critical point at $x = 0.7$ [5]. Subsequent muon-spin rotation measurements on the same crystals have proven that the magnetically ordered volume fraction at low- T decreases from 100% upon increasing Ca content x well before $T_C \rightarrow 0$ [7], indicating magnetic phase separation. Most interestingly, similar behavior has also been found near the pressure-driven first-order QPT in MnSi [7]. On the other hand, magnetization measurements on flux grown single crystals have shown FM order beyond $x = 0.8$ with a smooth crossover to spin-glass-like behavior at larger x , extending towards $x = 1$ [4]. Electrical resistivity measurements on thin films, prepared by pulsed-laser deposition have revealed an anomalous temperature dependence $\rho(T) = \rho_0 + A'T^{3/2}$ in a wide concentration range $0.8 \leq x \leq 1$ at temperatures

between 2 and 10 K, which resembles the NFL phase observed in MnSi under hydrostatic pressure. However, these thin films have a poor residual resistivity ratio, even for the undoped systems SrRuO_3 and CaRuO_3 and the experiments should be extended towards lower temperatures. In this paper, we report magnetization and electrical resistivity measurements on epitaxial $\text{Sr}_{1-x}\text{Ca}_x\text{RuO}_3$ thin films that have been grown using metal-organic aerosol deposition (MAD) [8].

2 Experimental Thin films of $\text{Sr}_{1-x}\text{Ca}_x\text{RuO}_3$, where grown by MAD on MgO and SrTiO_3 substrates [8]. In the former case, the larger lattice mismatch leads to a polycrystalline growth of islands, resulting in a substantial film roughness. By contrast, in the latter case epitaxial growth was obtained with very small values of the roughness detected by room temperature scanning tunneling microscopy. In this paper, we focus only on films grown on SrTiO_3 with in-plane dimensions of $10 \times 5 \text{ mm}^2$. Details of their preparation and structural characterization by X-ray diffraction and room-temperature scanning tunneling microscopy are reported in Ref. [8]. The thickness of each film has been determined by small-angle X-ray scattering and varies between 40 and 50 nm. Magnetization and electrical resistivity measurements at temperatures between 2 and 300 K were performed using Quantum Design MPMS and

PPMS systems, respectively. The electrical resistivity between 60 mK and 10 K has been determined in an adiabatic demagnetization cryostat on a microstructured film. Electrical contacts were made using silver paste.

3 Magnetization To determine the magnetization of the $\text{Sr}_{1-x}\text{Ca}_x\text{RuO}_3$ thin films, the background contribution of the SrTiO_3 substrate must be subtracted. A measurement on a plain substrate has revealed a diamagnetic magnetization with an additional Curie–Weiss contribution at low temperatures resulting from a small amount of magnetic impurities. While the substrate contribution to the total magnetization is small for FM samples below their Curie temperature, it dominates in the paramagnetic regime in particular for $x \leq 0.7$ at low temperatures. Since our analysis assumes similar substrate contributions for all samples, which, however, may be incorrect for substrates with differing amount of magnetic impurities, a substantial error arises at low temperatures and large Ca concentrations. Thus, the exact position of the QPT cannot be determined from these experiments. As estimate for T_C , we have analyzed the positions of the inflection points of $M(T)$ measured at $H = 1000$ Oe.

As displayed in Fig. 1, the so-derived T_C data indicate a clear and systematic evolution from a FM in ground state at $x = 1$ towards a paramagnetic ground state at $x = 0.8$, in good agreement with Refs. [6, 7]. For a closer analysis of the magnetic properties close to the FM QPT it would be required to measure for each film the substrate contribution *before* the synthesis and to explore the exact positions of $T_C(x)$ by Arrott-plot analysis.

4 Electrical resistivity We now turn to the temperature dependence of the electrical resistivity $R(T)$ of the $\text{Sr}_{1-x}\text{Ca}_x\text{RuO}_3$ thin films. Figure 2a displays normalized data at temperatures between 2 and 300 K for $x = 0$ and 1. Similar

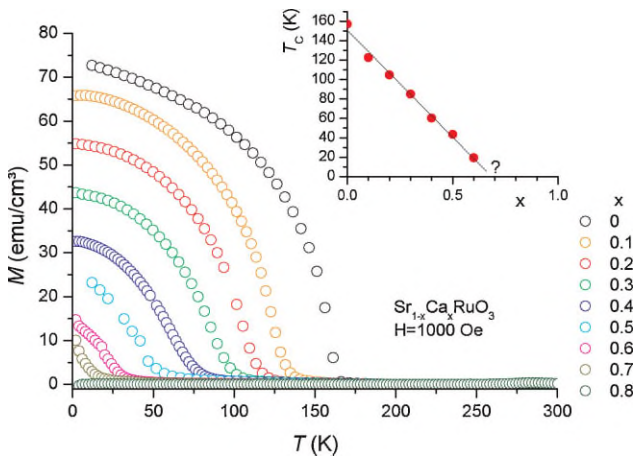


Figure 1 (online color at: www.pss-b.com) Temperature dependence of the magnetization of $\text{Sr}_{1-x}\text{Ca}_x\text{RuO}_3$ thin films. Each data set has been obtained at $H = 1000$ Oe after subtraction of the magnetization of a SrTiO_3 substrate. The inset displays the Curie temperature T_C versus x , derived from the inflection points in $M(T)$.

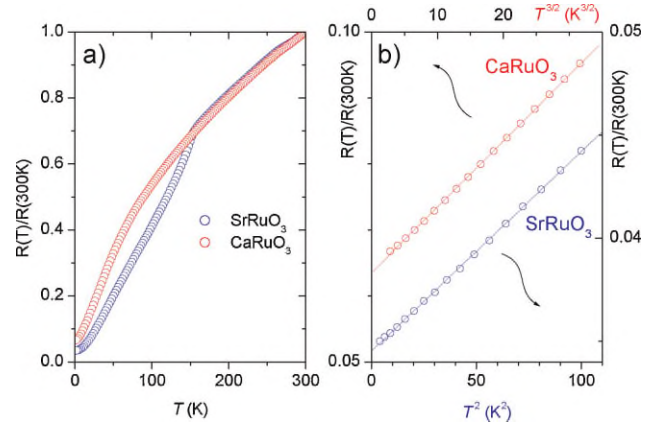


Figure 2 (online color at: www.pss-b.com) (a) Temperature dependence of the electrical resistivity of SrRuO_3 (blue circles) and CaRuO_3 (red circles) thin films. (b) Same data below 10 K plotted versus T^2 and $T^{3/2}$ for SrRuO_3 and CaRuO_3 , respectively.

measurements have been performed for all concentrations listed in Table 1. At low Ca concentrations, $x \leq 0.5$, sharp decreases in $R(T)$ are observed upon cooling through the respective Curie temperatures. For larger x , the signature becomes very weak and disappears. The residual resistivity ratios of 29 and 16 for $x = 0$ and 1, respectively, are much better compared to those reported in Refs. [6, 9] and indicate the good quality of the films. The lowest RRR value, is found for $x = 0.5$ (cf. Table 1), as expected from the maximum disorder due to the random Sr- and Ca substitution. The low- T data between 2 and 10 K have been fitted by a power-law temperature dependence, whose parameters are given in Table 1. Whereas a T^2 dependence, as expected for Fermi liquids, is found at $x < 0.7$, clear deviation is observed at larger Ca content. As shown in Fig. 2b for $x = 1$, the resistivity between 2 and 10 K could be described by a $T^{3/2}$ dependence, similar as found previously for thin films [6, 9] as well as single crystals in the same temperature range [4, 10]. The extension of the $x = 1$ data towards lower T is discussed later.

Table 1 Parameters derived from fits of the electrical resistivity of $\text{Sr}_{1-x}\text{Ca}_x\text{RuO}_3$ thin films at temperatures between 2 and 10 K according to $R(T) = R_0 + AT^n$.

sample	x	$A/R_{300\text{K}}$ (10^{-5} K^{-n})	n	RRR
T449	0	(7.86 ± 0.14)	2.09 ± 0.02	28.9
T648	0.1	(4.66 ± 0.53)	2.11 ± 0.04	4.2
T643	0.2	(6.30 ± 0.06)	2.05 ± 0.01	3.7
T642	0.3	(3.18 ± 0.80)	2.13 ± 0.05	3.6
T644	0.4	(9.51 ± 0.21)	2.01 ± 0.02	3.6
T414	0.5	(8.26 ± 2.1)	2.03 ± 0.09	2.9
T499	0.6	(25.8 ± 2.4)	1.89 ± 0.02	3.3
T498	0.7	(62.0 ± 8.8)	1.57 ± 0.07	3.2
T496	0.8	(73.9 ± 8.9)	1.48 ± 0.05	4.2
T495	0.9	(69.7 ± 9.5)	1.53 ± 0.02	6.1
T440	1.0	(79.4 ± 2.0)	1.51 ± 0.03	15.7

RRR denotes residual resistivity ratio $R_{300\text{K}}/R_0$.

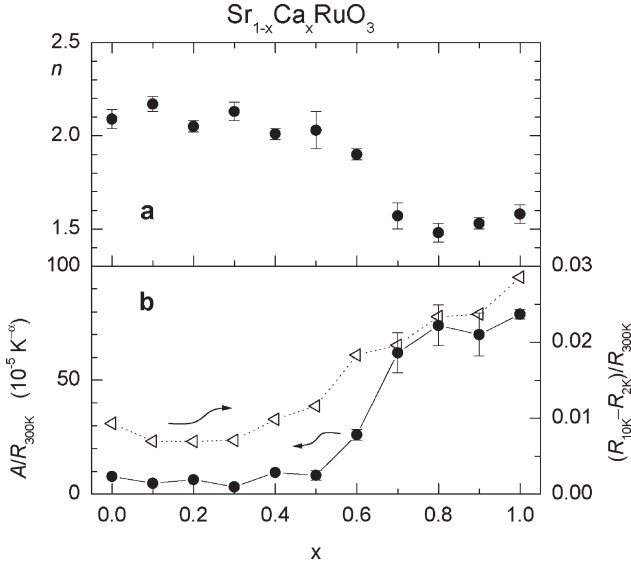


Figure 3 (a) Temperature exponent n derived from the fitting described in Table 1, versus Ca concentration in $\text{Sr}_{1-x}\text{Ca}_x\text{RuO}_3$. (b) Corresponding coefficient $A/R_{300\text{K}}$ (left axis) and resistance increase between 2 and 10 K, normalized to the room temperature resistance (right axis).

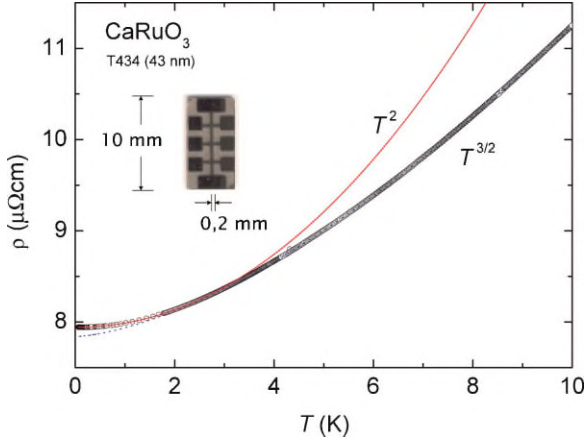


Figure 4 (online color at: www.pss-b.com) Low-temperature electrical resistivity of CaRuO_3 thin film number T434. The red solid and blue dotted lines display T^2 and $T^{3/2}$ behaviors, respectively. A photograph of the microstructured film with thickness of 43 nm is shown in the inset.

Figure 3 summarizes the concentration dependence of the fit parameters given in Table 1. Since it is difficult to compare values of the coefficient A obtained for varying exponents n , we also show the difference of the resistance between 2 and 10 K, normalized to the room temperature resistance. This latter property could be taken as a measure for the low- T scattering due to magnetic fluctuations in this system. A clear increase is found with increasing Ca-concentration suggesting enhanced magnetic fluctuations near the disappearance of long-range FM order. This is also

compatible with an enhanced specific heat coefficient ($\gamma \approx 80 \text{ mJ}/(\text{K}^2\text{mol-Ru})$ in CaRuO_3 [10]).

In order to study a possible NFL ground state in CaRuO_3 , the resistivity measurement has been extended down to 60 mK using a microstructured film shown in Fig. 4. Remarkably, we observe a crossover from $T^{3/2}$ to T^2 behavior below 2 K. This is in accordance with recent specific heat measurements on a high-quality single crystal, which show a constant specific heat coefficient at low temperatures [10]. Similar low- T measurements on thin films with $0.8 \leq x \leq 1$ are underway to determine the exact region in the $T-x$ phase diagram where the resistivity displays NFL behavior.

5 Conclusion The FM QPT in $\text{Sr}_{1-x}\text{Ca}_x\text{RuO}_3$ thin films has been studied using magnetization and electrical resistivity measurements. A clear and systematic evolution from $T_C = 160 \text{ K}$ at $x = 0$ towards $T_C \rightarrow 0$ at $x \approx 0.7$ is observed. The analysis of the temperature dependence of the electrical resistivity between 2 and 10 K suggests a broad concentration range in which NFL like behavior ($\Delta\rho \propto T^{3/2}$) is observed. However, the extension of the data for undoped CaRuO_3 down to 60 mK has revealed a crossover to Fermi liquid behavior $\Delta\rho \propto T^2$ at $T \leq 2 \text{ K}$.

Acknowledgements We thank C. Stingl and K. Winzer for their help with the low- T electrical resistivity measurement. Work supported by DFG through SFB 602.

References

- [1] S. S. Saxena, P. Agarwal, K. Ahilan, F. M. Grosche, R. K. W. Haselwimmer, M. J. Steiner, E. Pugh, I. R. Walker, S. R. Julian, P. Monthoux, G. G. Lonzarich, A. Huxley, I. Sheikin, D. Braithwaite, and J. Flouquet, *Nature* **406**, 587 (2000).
- [2] C. Pfleiderer, S. R. Julian, and G. G. Lonzarich, *Nature* **427**, 227 (2004).
- [3] N. Doiron-Leyraud, I. R. Walker, L. Taillefer, M. J. Steiner, S. R. Julian, and G. G. Lonzarich, *Nature* **425**, 595 (2003).
- [4] G. Cao, S. McCall, M. Shepard, J. E. Crow, and R. P. Guertin, *Phys. Rev. B* **56**, 321 (1997).
- [5] K. Yoshimura, T. Imai, T. Kiyama, K. R. Thurber, A. W. Hunt, and K. Kosuge, *Phys. Rev. Lett.* **83**, 4397 (1999).
- [6] P. Khalifah, I. Ohkubo, H. M. Christen, and D. G. Mandrus, *Phys. Rev. B* **70**, 134426 (2004).
- [7] Y. J. Uemura, T. Goko, I. M. Gat-Malureanu, J. P. Carlo, P. L. Russo, A. T. Savici, A. Aczel, G. J. MacDougall, J. A. Rodriguez, G. M. Luke, S. R. Dunsiger, A. McCollam, J. Arai, C. Pfleiderer, P. Böni, K. Yoshimura, E. Baggio-Saitovitch, M. B. Fontes, J. Larea, Y. V. Sushko, and J. Sereni, *Nature Phys.* **3**, 29 (2007).
- [8] M. Schneider, V. Moshnyaga, and P. Gegenwart, *Proceedings ICM 2009*, *J. Phys. Conf. Ser.*, to be published, arXiv:0905.4896 (2009).
- [9] L. Klein, L. Antognazza, T. H. Geballe, M. R. Beasley, and A. Kapitulnik, *Phys. Rev. B* **60**, 1448 (1999).
- [10] N. Kikugawa, L. Balicas, and A. P. Mackenzie, *J. Phys. Soc. Jpn.* **78**, 014701 (2009).